JMEPEG (2011) 20:244–249
DOI: 10.1007/s11665-010-9677-2

1059-9495/$19.00

Process Parameters in Resistance Projection Welding for Optical Transmission Device Package

Her-Yueh Huang and Kuang-Hung Tseng

(Submitted June 18, 2009)

The effects of main process parameters and electrode materials on joint quality (charging voltage and operating force) were investigated using detailed metallurgical examination and the helium leak test. The electrode materials used for resistance projection welding were brass and Cr-Cu alloy. The TO-Can components (cap and header) were nickel-coated SPCC steel. The results indicated that when the operating pressure increased, the electrode displacement increased, causing expulsion and distortion of the welds. The nugget area increased with the increase of charging voltage; however, it decreased with the increase of operating pressure. Results from the optical microscopy analysis showed that a larger acceptable welding range was achieved by using Cr-Cu electrodes. TO-Can in the acceptable and expulsion range successfully passed the helium leak rate of less than 5×10^{-8} mbar L/s. For commercial purposes, where dimensions have to be exact and without deformation, the TO-Can components produced in the expulsion zone cannot be used.

Keywords acceptable welding range, helium leak test, process parameter, resistance projection welding, transistor outline package

1. Introduction

Owing to an increased investment worldwide in the research and development of core technologies, the optoelectronics market has also experienced a huge growth in recent decades. Optical communication devices are now being used in almost areas of life. Without these devices, the information age would not even exist (Ref 1, 2). Today, the use of optical communication devices, inevitably followed by new technology, is ever increasing. The laser diode, one of the key devices for realizing high-performance optical networks, has been widely used for high-speed data writing/reading in communications or in players of optical discs (Ref 3).

Laser diode packaging technology includes three basic package types, namely metal can, dual-in-line (DIL), and butterfly (Ref 4). The most common packaging for laser diodes used in communication devices are metal cans style, commonly known as a transistor outline package or the TO-Can (Ref 5). TO packages include a cylindrical metal cap and metal header; a laser device is configured on the header to emit a single mode coherent light beam. Efficiency and reliability of the laser diode assembly depends on the alignment accuracy (Ref 6, 7). There is no doubt that the joining technology determines the TO-Can package quality. Sealed TO-Can packages are necessary for performance requirements and operational stability. In such packages, metal bonding techniques such as brazing or fusion welding are often used to provide a hermetic seal between the cap and the header, but they are costly and time consuming to manufacture (Ref 8). Therefore, resistance projection welding is used suitably for the fabrication of TO-Can assemblies, in which the heat necessary to produce a joint is generated by the Joule effect based on electrical resistance at the contact interface between the cap and the header. This process is also used extensively for joining most metals; either similar or dissimilar metal components. A typical resistance weld is broken down into three distinct periods. Each stage takes up a proportion of the total welding time (Ref 9, 10), as shown in Fig. 1. First, the squeeze time is when the coming together of the electrodes against the metal builds up to a specified pressure before the current is turned on. Next, weld time is when the current is turned on momentarily, which actually passes through the components because then the metals are hot enough to melt and fuse together to form a weld nugget. This is followed by the third, or hold time in which the current is turned off, but the pressure is still applied. The weld nugget cools, and the metals are forged under the pressure of the electrodes. Continued electrode pressure is applied till the weld solidifies, cools, and the weld nugget reaches its maximum strength.

The obtainment of the optimal hermetic metal package in resistance projection welding requires a thorough understanding of the process parameters. The effects of electrode materials and process parameters (including charging voltage and electrode force) on joint quality and nugget area were investigated. The experiment was focused on metallographic examination to estimate the acceptable welding range and run the helium leak test. Finally, information from resistance projection welding with high production rates and easy automation was obtained.

Her-Yueh Huang, Department of Materials Science and Engineering, National Formosa University, Yunlin 632, Taiwan; and **Kuang-Hung Tseng**, Department of Materials Engineering, National Pingtung University of Science and Technology, Pingtung 912, Taiwan. Contact e-mail: huanghy@nfu.edu.tw.

2. Experimental Procedure

A capacitor discharge-stored energy welding machine was used to seal a TO-Can component, as shown in Fig. 2. It controlled the voltage of the welding capacitors, and allowed extremely fast energy release with a large electric current in very short periods of time. The monitor signals were recorded together with the feedback from the peak current. The displacement signals were measured using a linear variable differential transformer (LVDT) sensor to directly reflect the position of the upper electrode in a welding cycle. The machine was equipped with a pneumatic pressure system. Welding, squeezing, and welding times were adjusted with the accessories on the machine. Before starting the resistance projection welding process, it is important to make sure that the setting on the welding machine is correct and that the cooling system's power is turned on. The charging voltage that was used varied from 150 to 350 kA with the welding time remaining constant at 4.4 ms. The operating pressure during the resistance projection welding process was set between 0.10 and 0.35 MPa at intervals of 0.05 MPa. The electrodes used in this study were brass (70 wt.%Cu-30 wt.%Zn) and Cr-Cu (15 wt.%W-85 wt.%Cu) alloy. The experimental material (TO-Can) was cold-rolled steel (SPCC) with an electrodeposited nickel coating of 10 μm formed by blanking and stamping. The specimen geometry and dimensions of the cap and header are shown in Fig. 3. The metallographic study was carried out using light optical microscopy on the transverse cross-sections of the weld joints passing through the weld nugget. All the specimens were prepared by cutting, grinding, and polishing to a finished grade of 0.3 μm; etching was done with nital.

Figure 4 is a schematic diagram of the helium leak detector. It consists of a test chamber, vacuum system, helium detector, and a display panel. In this system, a dry scroll pump was used to evacuate the test chamber through the vacuum valve, and then the chamber was connected to the detector through the sensing valve. The function of the adjusting valve was simply to test for leaks before starting the vacuum pump by closing all the valves except for the vacuum valve. In order to determine the leak rate of a TO-Can package, the specimen was placed in

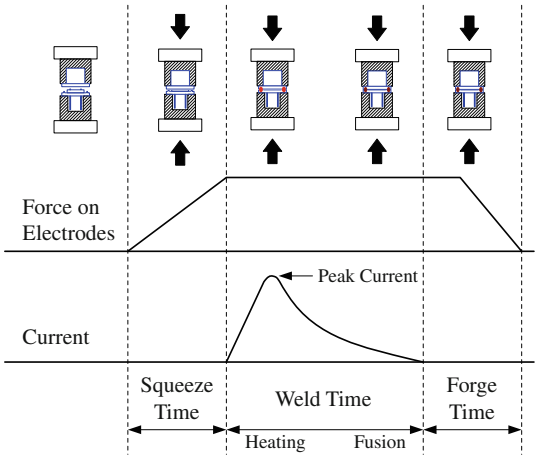

Fig. 1 Typical welding cycle for resistance projection welding

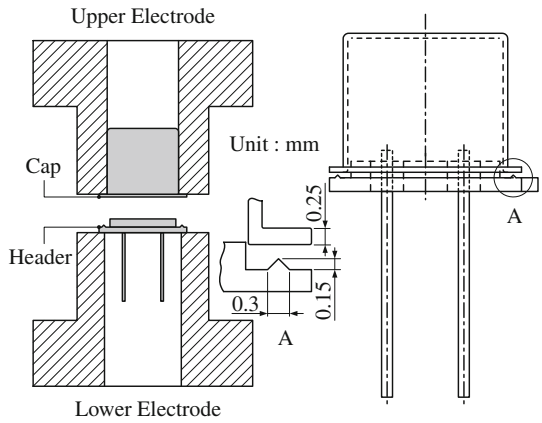

Fig. 3 Electrodes geometry and TO-Can dimension

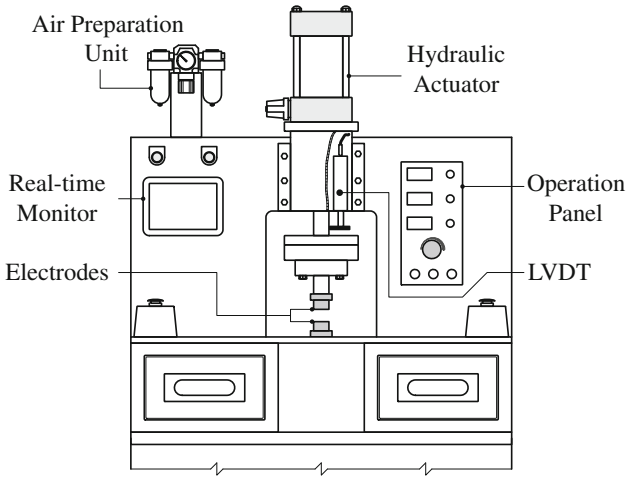

Fig. 2 Schematic representation of the experimental device for resistance projection welding

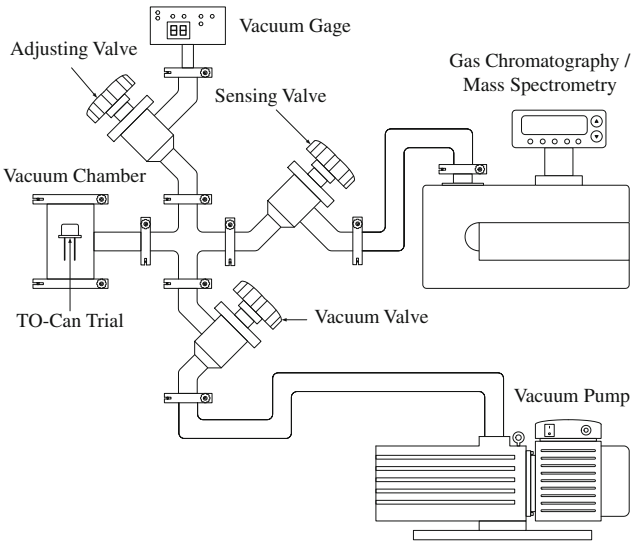

Fig. 4 Schematic diagram of the helium leak test

a pressurized chamber filled with helium for a period of time. In the event of a test specimen leak, i.e., TO-Can is unsealed; the pressurized helium would be forced through the opening into it. The chamber pressure is then released and the helium escaping from the TO-Can is transferred to the leak detector through the sensing valve. All of the helium that escapes from the TO-Can during the test is captured and measured. The leak detector background noise was 1.6×10^{-9} mbar L/s. Vacuum chamber pressure was 5.0×10^{-3} mbar and the specified time (bomb time) was 4 h. Response time, i.e., removal from the helium pressure chamber to detection, was 15 min.

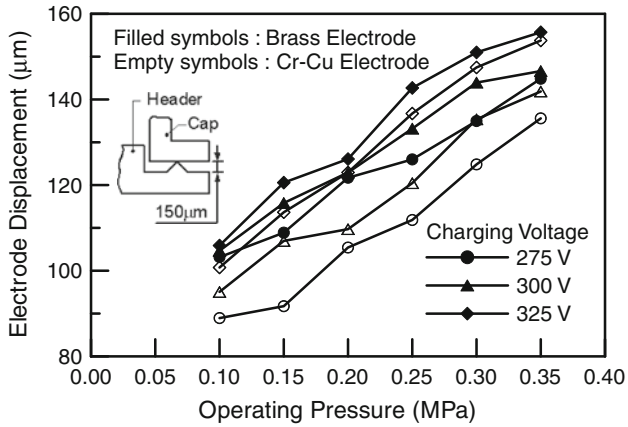

Fig. 5 Electrode displacement as function of operating pressure and charging voltage

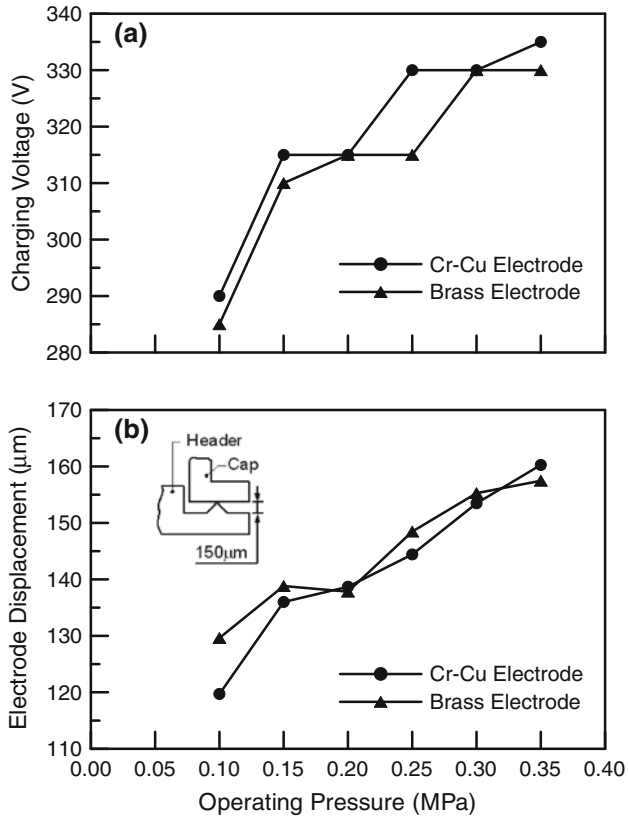

Fig. 6 (a) Effect of operating pressure on the maximum charging voltage not causing expulsion. (b) Relationship between electrode displacement and operating pressure under the maximum charging voltage not causing expulsion

3. Results and Discussion

3.1 Effect of Welding Parameters on Electrode Displacement

Electrode position can have a great affect on the finished weld quality. Electrode displacement information also indicates inadequate parameters (Ref 11), which results in an unacceptable TO-Can package. Too much pressure and voltage causes the electrode position to exceed the projection height, which may produce weld expulsion and unwanted part deformation. On the other hand, in the case of too little pressure and voltage, weld nugget will be small and weak. Figure 5 shows the influence of operating pressure and charging voltage on the electrode displacement. Electrode displacement increases with increase in operating pressure using either brass or Cr-Cu electrodes. This may be because of plastic deformation in the weld region. For the same operating pressure, an increase in charging voltage leads to an increase in electrode displacement. This is not surprising considering that higher charging voltage causes greater heat input, leading to molten metal flowing more easily and thus generating more displacement. In addition, the greatest electrode displacement should not exceed the projection height, i.e., 150 μm, and, therefore, it is used as a key quality criterion in packaging.

In this article, charging voltage and operating pressure are recognized as extremely important parameters to be taken into consideration to avoid expulsion. Figure 6(a) shows that the maximum charging voltage under the same operating pressure

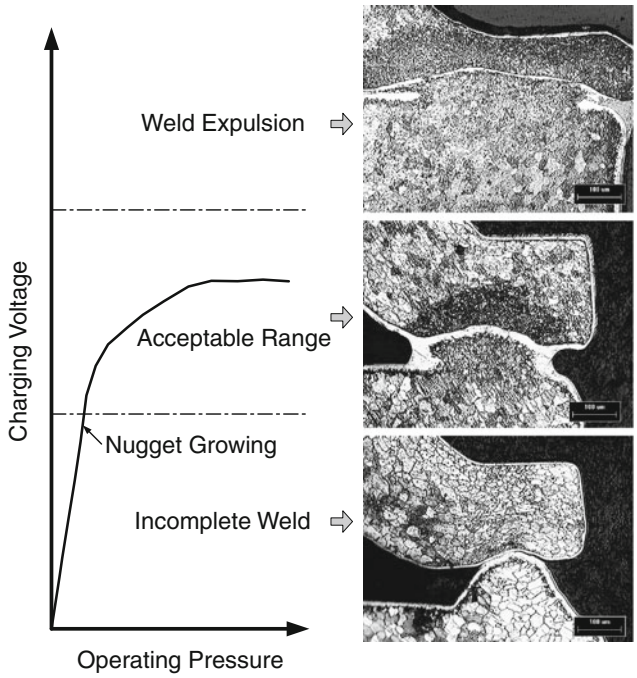

Fig. 7 Definition of acceptable and unacceptable welds in resistance projection welding

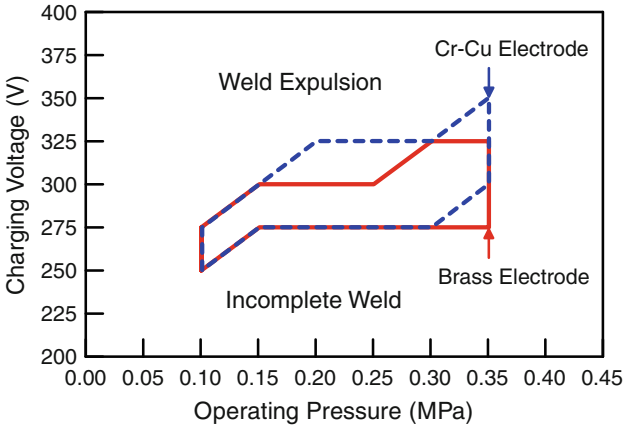

Fig. 8 Charging voltage and operating pressure vs. acceptable welding range

prevented weld expulsion. The charging voltage had to be increased as the operating pressure increased to avoid weld expulsion. It was because contact resistance decreased as the operating pressure increased. Low contact resistance results in low current density reducing heat generation and the size of the weld nugget (Ref 12, 13). Thus, a higher operating pressure requires a higher charging voltage to produce the best weld quality. Figure 6(b) shows the electrode displacement under the maximum charging voltage without weld expulsion. It was also found that the electrode displacement increased with the increase in operating pressure. This means that operating pressure and charging voltage constituted the prime electrode displacement parameters.

3.2 Estimation of Acceptable Welding Range

Successful resistance projection welding depends on the correct use of parameters. The charging voltage and operating

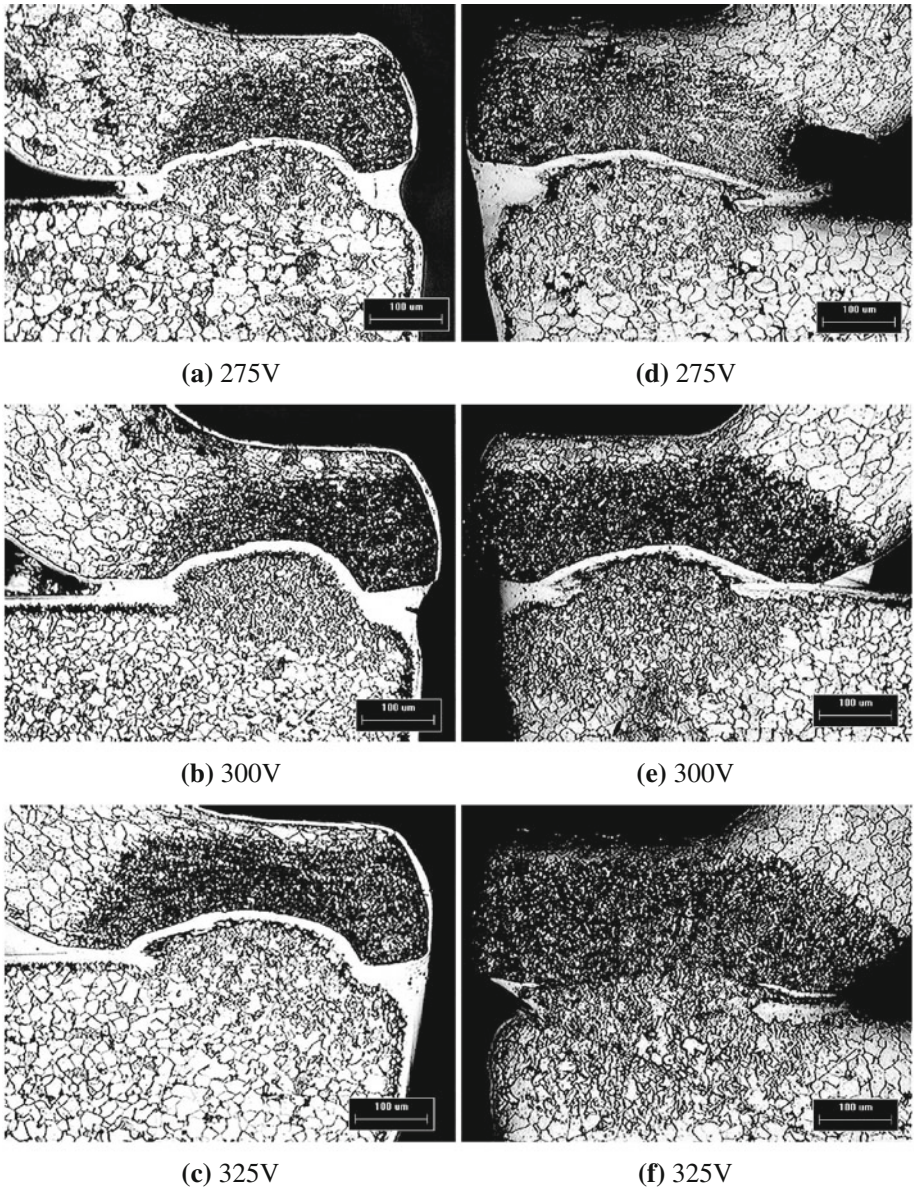

(a) 275V **(d)** 275V

(b) 300V **(e)** 300V

(c) 325V **(f)** 325V

Fig. 9 Cross sectional morphologies of welds. (a) 275 V, 0.3 MPa, Brass; (b) 300 V, 0.3 MPa, Brass; (c) 325 V, 0.3 MPa, Brass; (d) 275 V, 0.25 MPa, Cr-Cu; (e) 300 V, 0.25 MPa, Cr-Cu; and (f) 325 V, 0.25 MPa, Cr-Cu

pressure must be of sufficient magnitude to form a joint before projection collapse. In order to have a thorough understanding of the nugget formation process and the effects of different welding parameters, metallurgical examination of weld cross sections was used to evaluate weld quality. Definitions for incomplete, acceptable, and expulsion welds are given in Fig. 7. In order to determine the acceptable welding range, different weld parameters (operating pressure of 0.10-0.35 MPa and charging voltage of 250-350 V) were chosen to do a series of projection welding experiments, as shown in Fig. 8. In the acceptable welding range, the upper boundary represents weld expulsion, and the bottom boundary incomplete welding. Excessive heating tends to cause weld expulsion, metallurgical damage, and thermal deformation because of the charging voltage or operating pressure being too high. Incomplete weld joint occurred because of an incorrect setting of welding parameters i.e., voltage did not have enough heat input to completely fuse the projection. Besides, the acceptable welding range of the Cr-Cu electrode was bigger than that of the brass electrode. A wide acceptable welding zone indicated that obvious variations of parameters (such as operating pressure and charging voltage) in resistance projection welding could also be obtained while maintaining minimum weld joint quality. In contrast, a narrow acceptable welding range indicated minor variations in process parameters, thereby resulting in unacceptable welds.

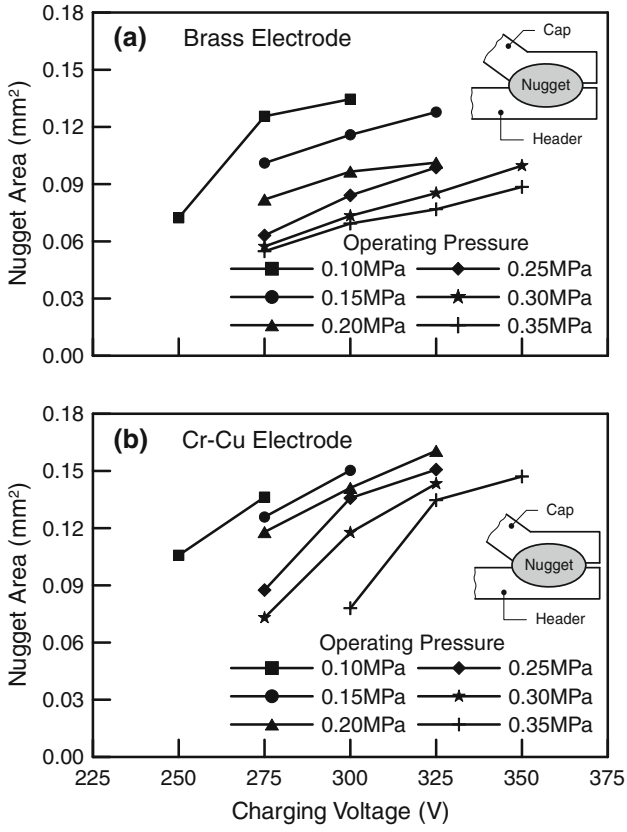

Fig. 10 Nugget area as function of charging voltage and operating pressure

3.3 Effect of Welding Parameters on Nugget Area

Figure 9 shows optical micrographs of the cross sections of projection welds made by the two types of electrode, brass and Cr-Cu. Under the same operating pressure, nugget area increased with the increase of the charging voltage. For the same charging voltage, projection collapse with the brass electrode was slower than the Cr-Cu electrode, and the Cr-Cu electrode needed a lower operating pressure. Therefore, the optimal nugget formation was obtained with a lower voltage and less force by using a Cr-Cu electrode.

The nugget area is an extremely important parameter, since it directly affects the quality of the projection weld. The relationship between nugget area and charging voltage at different operating pressures is shown in Fig. 10. The nugget area increased with the increasing charging voltage under different operating pressures. Besides, it also showed that operating pressure was an influential factor in projection welding. While charging voltage was fixed, increasing operating pressures seemed to decrease the nugget area. This phenomenon was due to operating pressure changing the contact area and thereby the contact resistance with a subsequent low current density which reduced heat generation and the area of the weld nugget (Ref 14-16).

3.4 Helium Leak Data Analysis

A suitable TO-Can sealing should prevent the ingress of external impurities, water vapor, and oxygen. Hermetic sealing of components, not only needs the optimal process parameters for resistance projection welding, but it also needs to pass the helium leak test.

According to the hermetic seal requirements of the military standard MIL-STD-883E method, the package must be capable of being sealed to achieve a leakage rate below 5×10^{-8} mbar L/s (Ref 17). At the bottom boundary of the acceptable welding range, all of the samples failed to create a hermetic seal, as shown in Fig. 11. Besides, samples passed the helium leak test successfully above or in the acceptable welding range. Below a leakage rate of 5×10^{-8} mbar L/s, the leakage rate decreased when the charging voltage increased, and a helium leakage rate as low as 1.5×10^{-8} mbar L/s was obtained at 350 V. In general, more charging voltage means more heat through the projection producing a tight weld. Charging voltage and operating pressure must be carefully controlled to produce

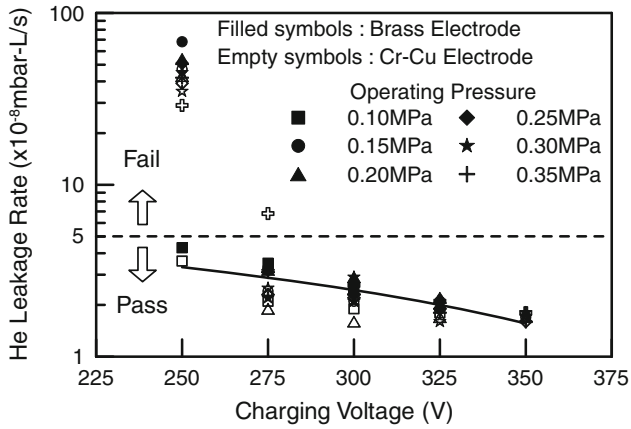

Fig. 11 Summary of the helium leak testing

commercial-grade TO-Can in terms of weld expulsion and distortion.

4. Summary

This research has shown that process parameters influence the joining quality of TO-Can package during resistance projection welding. The conclusions are summarised below:

1. An increase in operating pressure: However, this resulted in an increase in electrode displacement with the possibility of weld expulsion and distortion while exceeding projection height.
2. Acceptable welding ranges delineated the parameter boundary that produced welds with stable joints and leak-free sealing.
3. Nugget area increased with the increase of charging voltage. The decrease in contact resistance and current density resulted in a small nugget area, which usually occurs with an increase in operating pressure.
4. Although TO-Can in the expulsion zone successfully passed the helium leak, it cannot be used for commercial purposes because there is a dimension distortion.
5. The Cr-Cu electrode was found to have a wider acceptable welding range than the brass electrode. A narrow acceptable welding range meant that the brass electrode was more susceptible to process parameter variation and had more chance of failure.

References

1. I.P. Kaminow, The Third World in the Information Age, *Opt. Fiber Technol.*, 1998, **4**(4), p 339–344
2. J.S. Mayo, Global Communications in the Information Age, *IEEE Circuits Devices Mag.*, 1992, **8**(3), p 38–39
3. L. Li, The Advances and Characteristics of High-Power Diode Laser Materials Processing, *Opt. Lasers Eng.*, 2000, **34**, p 231–253
4. Y.C. Hsu, J.H. Kuang, Y.C. Tsai, and W.H. Cheng, Investigation and Comparison of Post-Weld-Shift Compensation Technique in TO-Can- and Butterfly-Type Laser-Welded Laser Module Packages, *IEEE J. Sel. Top. Quantum Electron.*, 2006, **12**(5), p 961–969
5. Y.C. Hsu, Y.C. Tsai, J.H. Kuang, and W.H. Cheng, Postweld-Shift-Induced Fiber Alignment Shifts in Laser-Welded Laser Module Packages: Experiments and Simulations, *J. Lightwave Technol.*, 2005, **23**(12), p 4287–4295
6. J.H. Kuang, M.T. Sheen, S.C. Wang, G.L. Wang, and W.H. Cheng, Post-Weld-Shift in Dual-in-Line Laser Package, *IEEE Trans. Adv. Packag.*, 2001, **24**, p 81–85
7. S.G. Kang, M.K. Song, S.S. Park, S.H. Lee, N. Hwang, H.T. Lee, K.R. Oh, G.C. Joo, and D. Lee, Fabrication of Semiconductor Optical Switch Module Using Laser Welding Technique, *IEEE Trans. Adv. Packag.*, 2000, **23**(4), p 672–680
8. A.L. Kovacs and D.F. Elwell, Integrated Brazed LTCC Packages, *Proceedings of the International Conference and Exhibition on Multichip Modules*, 1994, p 591–596
9. N. Kahraman, The Influence of Welding Parameters on the Joint Strength of Resistance Spot-Welded Titanium Sheets, *Mater. Des.*, 2007, **28**, p 420–427
10. A. Hasanbaşoğlu and R. Kaçar, Resistance Spot Weldability of Dissimilar Materials (AISI, 316L-DIN EN 10130–99 Steels), *Mater. Des.*, 2007, **28**, p 1794–1800
11. M. Jou, Real Time Monitoring Weld Quality of Resistance Spot Welding for the Fabrication of Sheet Metal Assemblies, *J. Mater. Process. Technol.*, 2003, **132**, p 102–113
12. D.Q. Sun, B. Lang, D.X. Sun, and J.B. Li, Microstructures and Mechanical Properties of Resistance Spot Welded Magnesium Alloy Joints, *Mater. Sci. Eng. A*, 2007, **460–461**, p 494–498
13. J. Xu, X. Jiang, Q. Zeng, T. Zhai, T. Leonhardt, J. Farrell, W. Umstead, and M.P. Effgen, Optimization of Resistance Spot Welding on the Assembly of Refractory Alloy 50Mo-50Re Thin Sheet, *J. Nucl. Mater.*, 2007, **366**, p 417–425
14. N. Harlin, T.B. Jones, and J.D. Parker, Weld Growth Mechanism of Resistance Spot Welds in Zinc Coated Steel, *J. Mater. Process. Technol.*, 2003, **143–144**, p 448–453
15. S. Aslanlar, The Effect of Nucleus Size on Mechanical Properties in Electrical Resistance Spot Welding of Sheets Used in Automotive Industry, *Mater. Des.*, 2006, **27**, p 125–131
16. P. Rogeon, P. Carre, J. Costa, G. Sibilia, and G. Saindrenan, Characterization of Electrical Contact Conditions in Spot Welding Assemblies, *J. Mater. Process. Technol.*, 2008, **195**, p 117–124
17. *Test Method Standard, Microcircuits*, Military Standard, MIL-STD-883E, Department of Defense, December 31, 1996